ARTICLES

Tungsten Carbide Nanocrystal Promoted Pt/C Electrocatalysts for Oxygen Reduction

Hui Meng and Pei Kang Shen*

State Key Laboratory of Optoelectronic Materials and Technologies, School of Physics and Engineering, Sun Yat-Sen University, Guangzhou 510275, P. R. China

Received: August 11, 2005; In Final Form: October 2, 2005

Tungsten carbide nanocrystals on carbon (W_2C/C) and tungsten carbide nanocrystals and Pt on carbon (Pt−W_2C/C) composite electrocatalysts were prepared by the intermittent microwave heating (IMH) method and tested for the electroreduction of oxygen in the acidic media for the first time. The results revealed that the tungsten carbide nanocrystal promoted Pt/C electrocatalyst was very active for ORR with the onset potential of 1.0 V vs SHE at ambient temperature that is over 100 mV more positive compared with that of traditional Pt/C electrocatalyst. The kinetic parameters were determined. The exchange current densities at both high and low overpotential regions are two orders higher for ORR on Pt−W_2C/C than that on Pt/C, showing a synergetic effect to improve the activity for ORR. The novel electrocatalysts show a poisoning resistant property toward methanol.

Introduction

The oxygen reduction reaction (ORR) is an important electrochemical reaction involved in low-temperature fuel cells,[1,2] oxygen sensors, metal−air batteries,[3] and the production of hydrogen peroxide.[4] The electroreduction of oxygen on the cathodic electrode in both acidic and basic solutions is always a slow reaction. The best catalyst Pt requires an overpotential of over 0.3 V under reasonable operating currents.[5,6] There has been considerable interest in the catalytic properties of tungsten carbides since they show exceptionally high activities similar to those of precious metal catalysts in a number of reactions,[7] such as electrooxidation of hydrogen, aldehydes, formic acid, and carbon monoxide.[8−11] However, to our knowledge no attempts have been made to evaluate the catalytic activity of nanocrystalline tungsten carbides for oxygen reduction. It is recognized that the particle size or the surface area of the catalyst is very critical for the catalytic reactions in terms of the activity and the utilization owing to the presence of a large number of surface atoms with properties different from those of bulk materials. We have demonstrated that the nanomaterials could be readily prepared by using the intermittent microwave heating (IMH) method.[12,13] Contrasting with other methods,[14−17] the present method is simple and rapid. Here we report that the same technique was used to prepare tungsten carbide nanocrystals on carbon and evaluated the electrocatalytic properties of the tungsten carbide nanocrystals and the tungsten carbide nanocrystal promoted Pt/C catalysts for oxygen reduction.

Experimental Section

Preparation of Tungsten Carbide Nanocrystals and Tungsten Carbide Nanocrystal Promoted Pt/C Electrocatalysts and the Electrodes. (*1*) *Tungsten Carbide Nanocrystals.* Tungsten powder (1 g) was added to 25 mL of aqueous solution containing 10 mL of 30 v/v % H_2O_2, 5 mL of 2-propanol, and 10 mL of water. The solution was left to rest for 24 h before 1 g of Vulcan XC-72 carbon powder (Cabot Corp., USA) was added. The mixture was treated in an ultrasonic bath to form uniformly dispersed ink. The ink was then dried in a microwave oven with a heating procedure of 5 s on and 5 s pause for six cycles. The dried powder was used as the precursor of tungsten carbides. The precursor powder in the quartz tube was further treated by the intermittent microwave heating procedure after 10 min of argon bubbling.

(*2*) *Tungsten Carbide Nanocrystal Promoted Pt/C Electrocatalysts.* Typically, 4 mg of as-prepared W_2C/C powder and 3.5 mg of 40 wt % Pt/C were added to 1 mL of 2-propanol. The well-mixed material was treated by IMH for 30 min, resulting in the further uniformly dispersed Pt−W_2C/C catalysts.

(*3*) *Electrodes.* The graphite rod with a diameter of 6 mm was used as electrode substrate and the top surface of the rod was pre-cleaned. Typically, 4 mg of catalysts was mixed with 1 mL of 2-propanol. The mixture was treated ultrasonically for 30 min for uniform dispersion. A quantity of mixture was then dropped onto the top surface of the graphite rod to produce electrodes with different catalyst loadings. Finally, a drop of 0.5 wt % Nafion solution was covered on top to prevent damage of the catalyst layer.

Characterization of Tungsten Carbide Nanocrystals and Tungsten Carbide Nanocrystal Promoted Pt Catalysts. The morphology and the particle size and distribution of the samples were studied by high-resolution transmission electron microscopy: JOEP JEM-2010 HRTEM (JEOL Ltd) operating at 200 kV. XRD measurements were carried out with a D/Max-IIIA diffratometer (Rigaku Co., Japan), using Cu Kα_1 (λ = 1.54056 Å) as the radiation source. Electrochemical measurements were performed at the VoltaLab 80 Universal Electrochemical Laboratory (Radiometer Analytical Company, France). A stan-

* Address correspondence to this author. E-mail: stdp32@zsu.edu.cn.

10.1021/jp054523a CCC: $30.25
Published on Web 11/10/2005

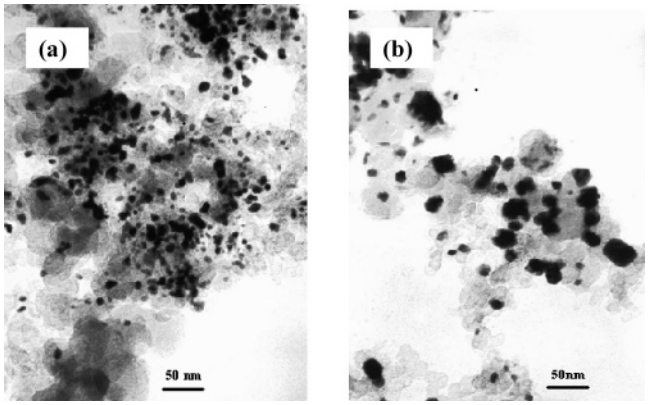

Figure 1. TEM images of the tungsten carbides: (a) 30 wt % W and (b) 40 wt % W.

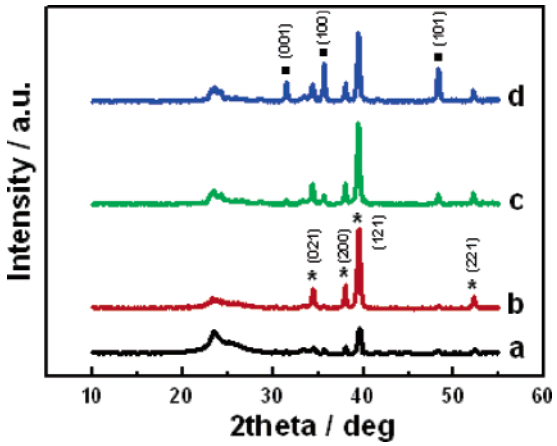

Figure 2. XRD patterns of the tungsten carbide nanocrystals prepared with the content of W of (a) 10, (b) 20, (c) 30, and (d) 40 wt %: ●, WC; ∗, W_2C.

dard three-electrode cell with separate anode and cathode compartments was used. A platinum foil and SCE electrodes were used as counter electrode and reference electrode, respectively. However, all potentials shown in the figures are against the standard hydrogen electrode (SHE). All the electrochemical measurements were carried out in a 0.5 mol dm^{-3} H_2SO_4 solution at 25 °C.

Results and Discussion

Figure 1a shows the typical transmission electron microscopic (TEM) images. The images indicate that the tungsten carbides prepared by the IMH method are nanometer particles. The average particle sizes are less than 10 nm when the ratios of W to C are controlled below 30 wt %, while the particles grow bigger at higher ratios (see Figure 1b). The particle size exceeds 20 nm at W:C = 1:1 (50 wt % W). The TEM images of Pt−W_2C/C are similar to that of W_2C/C and the discrimination of Pt and W_2C nanoparticles is difficult because of their similar darknes.[18]

The X-ray diffraction (XRD) determination confirmed that tungsten carbides prepared by the present method are nanocrystals. The XRD patterns of the tungsten carbide nanocrystals with different ratios of W to C are shown in Figure 2. The peaks shown in the figure are identified as that of pure W_2C at the percentage of W less than 30 wt %. Further increase in the content of W results in the formation of WC. XRD analyses clearly showed the existence of crystalline WC and W_2C. For W_2C, the 2θ of 34.32, 37.96, 39.40, and 52.12 with the d values of 2.6107, 2.3683, 2.2850, and 1.7533 correspond to the (021), (200), (121), and (221) peaks. For WC, the 2θ of 31.36, 35.56, and 48.24 with the d values of 2.8500, 2.5224, and 1.8849 correspond to the (001), (100), and (101) peaks. The ratios of WC to W_2C would increase with the increase in the heating time. Figure 3 compares the XRD patterns of W_2C/C and Pt−W_2C/C. It is clear that the XRD pattern of Pt−W_2C/C combines the crystalline features of Pt and W_2C, indicating the coexistence of both.

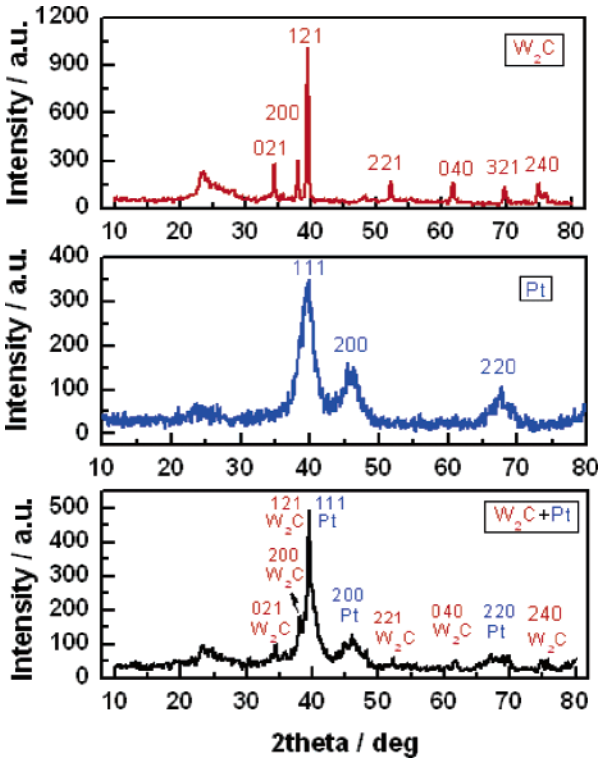

Figure 3. Comparison of XRD patterns of W_2C/C, Pt/C, and Pt−W_2C/C.

The tungsten carbide nanocrystals have no activity for oxygen reduction in acidic solution (see Figure 4a). This means that the pure tungsten carbide nanocrystals could not be used as electrocatalysts for ORR. However, the addition of tungsten carbide nanocrystals to Pt/C significantly improved the ORR performance, which is much better than that on pure Pt/C electrocatalysts (Figure 4a). The oxygen electroreduction started at 1.0 V on the nanocrystalline W_2C promoted Pt/C electrode instead of the 0.88 V on Pt/C electrode. As we know that the Tafel equation is valid at charge-transfer control condition, $\log -j = \log j_o - (\alpha_c nF/2.3RT)\eta$.[19] Re-plotting the data in Figure 4a gives the Tafel plots as shown in Figure 4b. The plots show two well-defined linear regions for both Pt/C and Pt−W_2C/C catalysts with the similar slopes. The slopes at the low current density region (region 1) for Pt/C and Pt−W_2C/C are −62 and −66 mV per decade respectively, and the slopes are −121 and −126 mV per decade at the high current density region (region 2). A Tafel plot showing two linear segments with slopes of about −60 mV per decade and −120 mV per decade has usually been reported for the O_2 reduction reaction on platinum electrode in acidic medium. The change in the Tafel slope is attributed to the influence of different adsorption and different rate-determining steps over the potential ranges investigated and is related exclusively to the change in the mechanism/kinetics of the oxygen reduction. The existence of two slopes is explained in terms of the coverage of the electrode surface by adsorbed oxygen. The Tafel slope is −60 mV per decade at low overpotential and a high coverage of adsorbed oxygenated

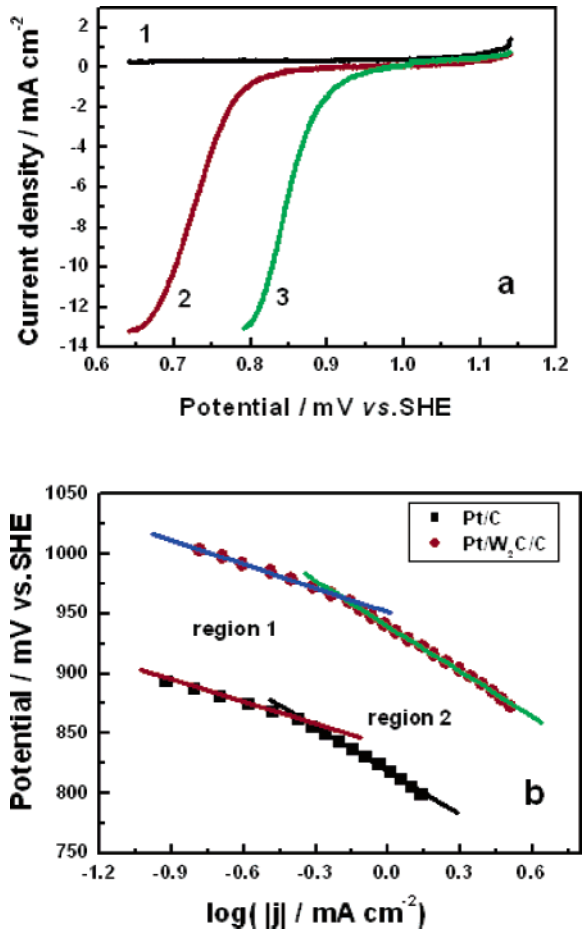

Figure 4. (a) Linear sweep curves of oxygen reduction on different catalysts in O_2 saturated 0.5 mol dm^{-3} H_2SO_4 solution at 25 °C: curve 1, 80 μg of W_2C; curve 2, 80 μg of Pt; curve 3, 40 μg of Pt + 80 μg of W_2C; sweep rate, 2 mV s^{-1}. (b) Tafel slopes for ORR on Pt/C and Pt−W_2C/C electrocatalysts.

intermediate species. The main adsorbed intermediate species are probably O_{ads}, OH_{ads}, and O_2H_{ads}. They are in quasiequilibrium and their surface concentrations vary linearly with potential and pH according to the Temkin isotherm. At high overpotential and a low coverage, the Tafel slope is −120 mV per decade and the surface concentrations of adsorbed intermediate species vary according to the Langmuir isotherm. As a generally accepted reaction mechanism,[20−23] the first step in the overall reaction path is the adsorption of O_2 on the Pt surface:

$$O_2 \rightarrow O_{2(ad)}$$

which is followed by the rate-determining step:

$$O_{2(ad)} + e^- \rightarrow O_{2(ad)}^-$$

The −120 mV Tafel slope implies that the first charge transfer step is likely to be the rate-determining step.[22,24−26]

The values of the exchange current densities may be obtained by extrapolation of the Tafel line to the equilibrium potential, E_{eq}, for the O_2 reduction (1.23V vs SHE). The exchange current densities for O_2 reduction on two electrodes corresponding to each Tafel slope are shown in Table 1. The exchange current densities in two regions are around 10^{-10} and 10^{-7} A cm^{-2} on different electrocatalysts reported in the literature.[20,27−34] In this work, the exchange current densities of oxygen reduction on Pt−W_2C/C were almost two orders of magnitude higher than that on Pt/C. This will significantly improve the oxygen

TABLE 1: Comparison of Kinetic Parameters for ORR on Pt/C and Pt−W_2C/C Electrocatalysts

catalyst	onset potential/ mV vs SHE	Tafel slope/ mV $decade^{-1}$		exchange current density/A cm^{-2}	
		region 1	region 2	region 1	region 2
Pt/C	887	−62	−121	5.25×10^{-10}	3.16×10^{-7}
Pt−W_2C/C	1002	−66	−126	4.7×10^{-7}	5.01×10^{-5}

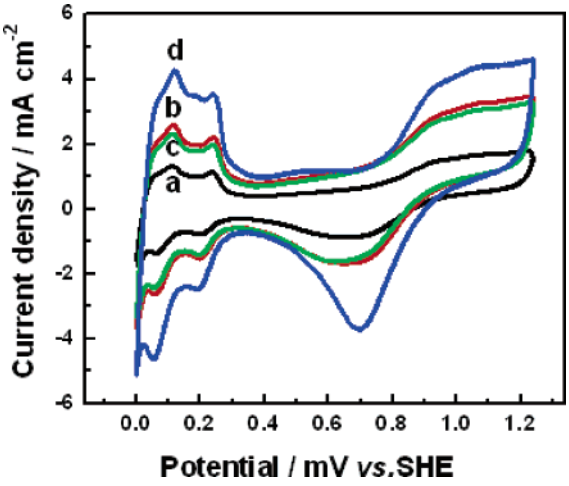

Figure 5. Cyclic voltammograms of (a) 40 μg of Pt, (b) 80 μg of Pt, (c) 40 μg of Pt + 80 μg of W_2C, and (d) 80 μg of Pt + 80 μg of W_2C electrocatalysts in 0.5 mol dm^{-3} H_2SO_4 at 25 °C; scan rate = 50 mV s^{-1}.

reduction activity and substantially increase the power output of a fuel cell since the efficiency of fuel cells is limited on the cathode side by the ORR. By analogy with the mechanism in enhancement of ORR activity proposed by Markovic and coworkers,[21] the enhancement of ORR activity on Pt−W_2C/C electrocatalyst is probably due to (i) modification of the electronic structure of Pt (5-d orbital vacancies), (ii) a change in the physical structure of Pt (Pt−Pt bond distance and coordination number), and (iii) adsorption of oxygen containing species from the electrolyte onto the tungsten carbides.

We also checked the electrochemically active areas of both electrodes by cyclic voltammetry to confirm the synergistic effect of the Pt−W_2C/C electrocatalyst. Figure 5 shows the typical cyclic voltammograms of Pt/C electrodes with or without W_2C in a 0.5 mol dm^{-3} H_2SO_4 background solution at a scan rate of 50 mV s^{-1}. The perfect curves clearly show that the hydrogen adsorption/desorption peaks (or areas) are proportional to the amount of Pt on the electrode. It is worth noting that the electrode b and electrode c which gave the oxygen reduction curve 2 and curve 3 in Figure 4 are hardly different despite the Pt loading on the pure Pt/C electrode being double that on the Pt−W_2C/C electrode. On the other hand, the increased magnitude in the hydrogen adsorption/desorption areas is almost the same as the increases in the amount of Pt, indicating a well-structured electrode and high utilization of catalyst. Therefore, we can conclude that the increase in the electrochemical activity is not due to the increase in the surface area of the electrode since the true surface areas are almost the same for the two electrodes. This can be explained in that the synergetic effect between the tungsten carbide nanocrystals and Pt might exist at the interface such that the tungsten carbides intervene in the catalytic process.

Direct methanol fuel cells (DMFCs) have recently emerged as the technology of choice for low-temperature power applications. For DMFCs methanol is used as the fuel instead of hydrogen. The interest with methanol is that methanol has a

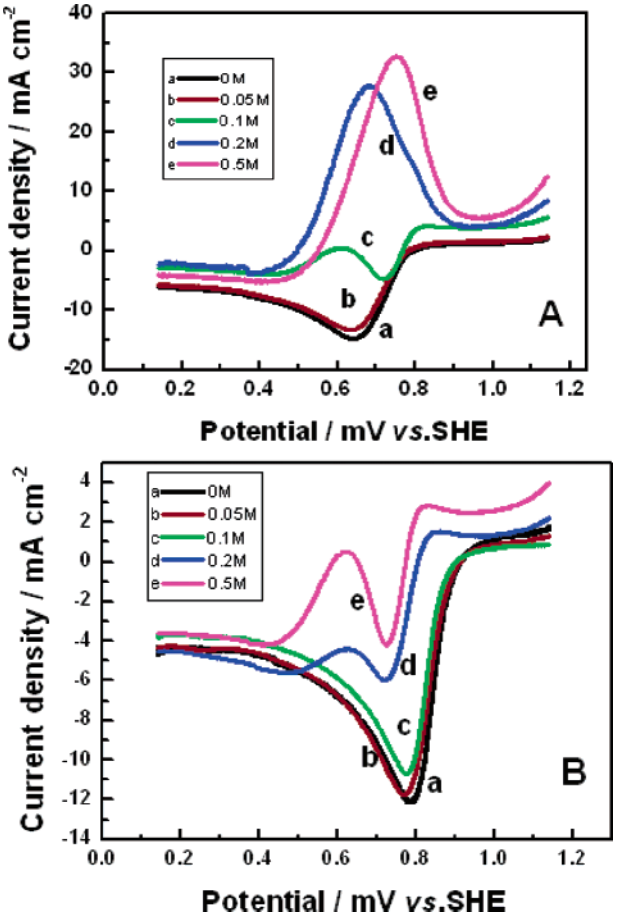

Figure 6. (A) CVs of ORR on Pt/C in an O_2 saturated 0.5 mol dm^{-3} H_2SO_4 solution with different methanol concentrations at 25 °C; sweep rate = 2 mV s^{-1}. (B) CVs of ORR on Pt−W_2C/C at the same conditions.

similar distribution infrastructure to petroleum. A major operating constraint is the methanol crossover from the anode to the cathode, which causes a loss in fuel and also the formation of a mixed potential at the cathode, leading to reduced cell performance.[35,36] It is desirable to develop electrocatalysts with a high selectivity toward oxygen reduction. On the other hand, the current DMFCs use high loading of expensive Pt as electrocatalyst, which severely prohibits their broad commercialization. Therefore, the effect of methanol in the supporting electrolyte on the ORR on two electrodes was studied to better understand the depolarizing effects of methanol crossover in the DMFC by comparing the electrocatalytic activities of tungsten carbide nanocrystal promoted Pt/C electrocatalyst and traditional Pt based electrocatalysts.

Shown in Figure 6A are the results for ORR in the presence of methanol on the Pt/C electrode. It is obvious that the activity for ORR was significantly reduced in the presence of methanol. The ORR was totally depressed at concentrations of methanol over 0.1 mol dm^{-3}. The competitive adsorption of oxygen and methanol on the surface of Pt results in a mixed potential. The electrode reaction is dominant for the methanol oxidation at higher methanol concentrations and limited dissolved oxygen since Pt is active for both oxygen and methanol.

The effect of methanol on the performance of the Pt−W_2C/C electrode for the ORR is shown in Figure 6B. From the cyclic voltammograms we can find that the effect of methanol on the electrode activity for oxygen reduction on the Pt−W_2C/C electrode was tremendously reduced compared with that on the Pt/C electrode. The ORR is still the dominant reaction at the concentration of methanol up to 0.5 mol dm^{-3} even when the onset potential moved to a more negative position. The results indicate that the tungsten carbide nanocrystal promoted Pt/C electrocatalyst is a selective electrocatalyst toward oxygen reduction.

Conclusion

Tungsten carbide nanocrystals on carbon (W_2C/C) and tungsten carbide nanocrystals and Pt on carbon (Pt−W_2C/C) composite electrocatalysts were prepared by the IMH method and tested for the electroreduction of oxygen in acidic media for the first time.

The results revealed that the tungsten carbide nanocrystal promoted Pt/C electrocatalyst is very active for ORR with the onset potential of 1.0 V vs SHE at ambient temperature that is over 100 mV more positive compared with that of traditional Pt/C electrocatalyst. This will significantly increase the power output for a fuel cell since the efficiency of fuel cells is limited by the cathode side for the ORR. The kinetic parameters were determined and the exchange current densities both at high and low overpotential regions are two orders of magnitude higher on Pt−W_2C/C than that on Pt/C, showing a synergetic effect to improve the activity for ORR. The unique properties of the selectivity and immunity to methanol of the novel electrocatalysts are favorable for potential applications in direct alcohol fuel cells, alcohol monitors, and metal−air batteries.

Acknowledgment. This study was supported by the National Natural Science Foundation of China (20476108), Guangdong Province Natural Science Foundation (01105500), Guangdong Science and Technology Key Project (2004A11004001), and China National 863 Program (2003AA517050).

References and Notes

(1) Nissinen, T. A.; Kiros, Y.; Gasik, M.; Leskela, M. *Chem. Mater.* **2003**, *15*,
(2)
(3) Jaouen, F.; Marcotte, S.; Dodelet, J. P.; Lindbergh, G. *J. Phys. Chem. B* **2003**, *107*, 1376.
(4) Weidenkaff, A.; Ebbinghaus, S. G.; Lippert, T. *Chem. Mater.* **2002**, *14*, 1797.
(5) Li, Y. J.; Chang, C. C.; Wen, T. C. *Ind. Eng. Chem. Res.* **1996**, *35*, 4767.
(6) Schmidt, T. J.; Stamenkovic, V.; Radmilovic, V.; Markovic, N. M.; Ross, P. N. *J. Phys. Chem. B* **2002**, *106*, 4181.
(7) Lamy, C.; Lima, A.; LeRhun, V.; Delime, F.; Coutanceau, C.; Léger, J. M. *J. Power Sources* **2002**, *105*, 283.
(8) Boudart, M.; Levy, R. *Science* **1973**, *181*, 547.
(9) McIntyre, D. R.; Burstein, G. T.; Vossen, A. *J. Power Sources* **2002**, *107*, 67.
(10) Barnett, C. J.; Burstein, G. T.; Kucernak, A. R. J.; Williams, K. R. *Electrochim. Acta* **1997**, *42*, 2381.
(11) Baresel, D.; Gellert, W.; Heidemeyer, J.; Scharner, P. *Angew. Chem.* **1971**, *10*, 194.
(12) Binder, H.; Kohling, A.; Kuhn, W.; Sandstede, G.. *Angew. Chem.* **1969**, *8*, 757.
(13) Shen, P. K.; Tian, Z. Q. *Electrochim. Acta* **2004**, *49*, 3107.
(14) Xu, C. W.; Shen, P. K. *Chem. Commun.* **2004**, 2238.
(15) Delannoy, L.; Giraudon, J. M.; Granger, P.; Leclercq, L.; Leclercq, G. *J. Catal.* **2002**, *206*, 358.
(16) Nartowski, A. M.; Parkin, I. P.; Mackenzieb, M.; Cravenb, A. J. *J. Mater. Chem.* **2001**, *11*, 3116.
(17) Palmquist, J. P.; Czigany, Zs.; Oden, M.; Neidhart, J.; Hultman, L.; Jansson, U. *Thin Solid Films* **2003**, *444*, 29.
(18) Oxley, J. D.; Mdleleni, M. M.; Suslick, K. S. *Catal. Today* **2004**, *88*, 139.
(19) Pino L.; Vita A.; Cordaro M.; Recupero V.; Hegde M. S. *Appl. Catal. A* **2003**, *243*, 135.
(20) Pletcher, D.; Walsh, F. C. *Industrial Electrochemistry*; Blackie Acdemic & Professional: London, UK, 1993; p 12.
(21) Antoine, O.; Bultel, Y.; Durand, R. *J. Electroanal. Chem.* **2001**, *499*, 85.

(22) Stamenkovic, V.; Schmidt, T. J.; Ross, P. N.; Markovic, N. M. *J. Electroanal. Chem.* **2003**, *554*−*555*, 191.
(23) Markovic, N. M.; Gasteiger, H. A.; Grgur, B. N.; Ross, P. N. *J. Electroanal. Chem.* **1999**, *467*, 157.
(24) Tur'yan, Y. I.; Gorenbein, P.; Kohen, R. *J. Electroanal. Chem.* **2004**, *571*, 183.
(25) Liu, B.; Bard A. J. *J. Phys. Chem. B* **2002**, *106*, 12801.
(26) Tammeveski, K.; Tenno, T.; Claret, J.; Ferrater, C. *Electrochim. Acta* **1997**, *42*, 893.
(27) Tammeveski, K.; Arulepp, M.; Tenno, T.; Ferrater, C.; Claret, J. *Electrochim. Acta* **1997**, *42*, 2961.
(28) Kucernak, A.; Jiang, J. H. *Chem. Eng. J.* **2003**, *93*, 81.
(29) Chen, S. L.; Kucernak, A. *J. Phys. Chem. B* **2004**, *108*, 3262.
(30) Lima, F. H. B.; Ticianelli E. A. *Electrochim. Acta* **2004**, *49*, 4091.
(31) Perez, J.; Gonzalez, E. R.; Ticianelli, E. A. *Electrochim. Acta* **1998**, *44*, 1329.
(32) Yu, E. H.; Scott, K.; Reeve, R. W. *Fuel Cells* **2003**, *3*, 169.
(33) Huanga, K. L.; Holsenb, T. M.; Selmanc, J. R.; Choud, T. C. *J. Power Sources* **2005**, *142*, 243.
(34) Basura, V. I.; Beattie, P. D.; Holdcroft, S. *J. Electroanal. Chem.* **1998**, *458*, 1.
(35) Singh, R. N.; Lal, B.; Malviya, M. *Electrochim. Acta* **2004**, *49*, 4605.
(36) Sundmacher, K.; Scott, K. *Chem. Eng. Sci.* **1999**, *54*, 2927.
(37) Steele, B. C. H.; Heinzel, A. *Nature* **2001**, *414*, 345.